Environmental Consequences of Nuclear War Volume I:
Physical and Atmospheric Effects
A. B. Pittock, T. P. Ackerman, P. J. Crutzen,
M. C. MacCracken, C. S. Shapiro and R. P. Turco

CHAPTER 4
Atmospheric Processes

4.1 INTRODUCTION

As an introduction to Chapters 5 and 6, which present the atmospheric response to the smoke and dust injections described in Chapter 3, this chapter focuses on the physical processes in the atmosphere that interact with the injected aerosol. The first section is concerned with plume rise and mesoscale processes that affect the early dispersion of the injected material. The next section treats physical processes such as radiative transfer and atmospheric transport, which interact with aerosol on the longer time scales of weeks to months. The last section discusses briefly geophysical analogues and their relevance to the problem of climatic disturbance following a nuclear war. This chapter should be seen as a bridge between the preceeding chapters, which are primarily concerned with determining the quantity and type of material injected into the atmosphere, and the following chapters, which are primarily concerned with the longer time scale response to the injection. In addition, it attempts to provide some perspective on the importance of various physical processes in determining the climatic response and on the degree to which these processes can be simulated in current climate models.

4.2 SHORT TERM ATMOSPHERIC RESPONSE TO SURFACE FIRES

Fires of the intensity and areal extent of those likely to occur in the aftermath of a modern thermonuclear exchange, and the plumes associated with them, are beyond normal experience. The wildfires that occur periodically in forests and grasslands are fundamentally unlike those that would result from a nuclear detonation. Whereas usual wildfires are set from a single or limited number of iginition points, a nuclear detonation can simultaneously ignite tens or hundreds of square kilometers of forest, brush, and grass, thereby inducing fires of areal extent much larger than ever observed before (NRC, 1985). Some closer approximations to what might occur are the fires, firestorms, and associated smoke plumes caused by conventional and nuclear bombings of cities during the Second World War. The conventional

incendiary bombings of Dresden and Hamburg both resulted in intense fire storms. Although documented observations of the resulting fires and fire plumes are sketchy, anecdotal evidence indicates that smoke plumes reached 6–12 km in height (NRC, 1985). The Hamburg fire, although covering an area of only 12 km^2, had an estimated heat output of 1.7×10^6 MW and produced a smoke plume that reached altitudes ranging from 9–12 km (Ebert, 1963; Carrier et al., 1983).

Following the nuclear detonations over both Hiroshima and Nagasaki, observations of smoke were again limited. The early morning bombings occurred in early August, 1945, at which time the local maritime atmosphere was conditionally unstable. Because of topographical influences, the resulting fire in Nagasaki was less extensive than that in Hiroshima (see Chapter 1). In both cities, a large cumulonimbus cloud formed over the the fire that produced a "black rain" at the surface; at Hiroshima, the rain began within 20 minutes of the blast. Molenkamp (1980) estimates that 5–10 cm of rain fell in parts of Hiroshima in a 1–3 hour period, while the amount was somewhat less in Nagasaki (Ishikawa and Swain, 1981).

These historical fire events are small compared to those that could occur today with modern weapons. Whereas the Hamburg firestorm covered 12 km^2 with an average heat flux of about 14×10^4 W/m^2 (Ebert, 1963; Carrier et al., 1983), a current strategic nuclear weapon is capable of simultaneously igniting a city of several hundred square kilometers. Larson and Small (1982) have estimated that fuel loadings in some city centers can approach that of the pre-firestorm Hamburg fuel density of 470 kg/m^2 over a region of 3–13 km^2. They also estimated fuel loadings of 110 kg/m^2 over a substantially larger region of 47–100 km^2 surrounding the city center. Because a nuclear detonation could ignite the entire region simultaneously, total heat fluxes in a modern city could reach as high as 10^5 W/m^2 (equivalent to about 10^7 MW over the region) if a large fraction of the combustible material were to burn in 3–6 hours. (It is not certain that all of the material would burn, especially in the regions of heaviest debris; see Chapter 3, and Appendix 3A.) Such strong heat sources, which are roughly 10 to 100 times greater than the amount of solar radiation absorbed at the ground, could produce deep, often precipitating, atmospheric plumes that would inject smoke, dust, and moisture aloft.

4.2.1 Fire Induced Convective Plumes

The majority of nuclear weapon strategic targets lie in regions where, during the months of May–September, the atmosphere is likely to be conditionally unstable for moist convection most of the time. During March–April, and October–November, the atmosphere above the majority of the targets probably has sufficient moisture to feed convection if large and unusual sur-

face heat sources occur. In the remaining months of December–February, at least 50% of the targets may be in a conditionally unstable environment or possess enough moisture to supply unstable moist convection with a large surface heat flux. Therefore, over much of the year and in many locations, smoke resulting from large surface fires would be likely to enter a cumulonimbus cloud that is supported or triggered by the fire induced heat flux.

Fire induced moist convection could be somewhat more intense than natural moist convection for a given time and locality since it is augmented by the surface heat source. In fact, the heat flux of an intense, massive fire could be comparable to that which drives an intense cumulonimbus storm (which may have latent heat fluxes aloft exceeding 10^5–10^6 W/m^2 at mid levels over a region of 10–25 km^2). If heat fluxes are less than about 10^4 W/m^2, strong convection might not ocur. Smoldering fires would tend to inject smoke only into the boundary layer. In general, natural deep convective systems are found preferentially to detrain (release to the enviroment) most of their mass near the tropopause level (Yanai et al., 1973; Knupp, 1985). Hence, as a first approximation, it can be expected that deep moist convection induced by flaming fires would deposit much of the smoke carried up by the cloud into the region just below, or possibly just above, the tropopause (excepting, of course, for that smoke which is removed from the cloud by scavenging processes; see Chapter 3 for a discussion of scavenging mechanisms).

As with natural convective plumes, dynamic interactions with local winds and vertical wind shear can result in a helical and inertially stabilized plume updraft (Lilly and Gal Chen, 1983). For fires that persist for a period of several hours, a strong inward spiraling surface vortex might develop that would fan and further enhance the fire. There was evidence of such a whirlwind in the Hamburg firestorm, although not in the other mass fire cases.

Unlike natural moist convection, cumulonimbus clouds occurring in conjunction with surface fires would contain extremely high levels of pollutants (dust, smoke, debris, etc.) that could alter their microphysical development, which in turn could affect the plume development. Much higher than normal CCN (cloud condensation nuclei) concentrations might be produced, resulting in the formation of many very small droplets and preventing the formation of raindrops by autoconversion (growth to large drops by coalescence of smaller cloud droplets). This is probably not an important modification since raindrop formation by autoconversion is rare over continental regions, even with present background levels of pollutants and CCN. Other cloud microphysical effects may be anticipated as well. If the pollutants act effectively as ice nuclei (silicate is a primary ice nucleus) in addition to CCN, ice nucleation by condensation freezing could be augmented. This may lead to larger than normal ice crystal production rates in portions of the cloud above -20°C (where depositional nucleation rates are normally small) and

perhaps smaller than normal ice crystal sizes overall. It is unclear, however, whether this would augment or weaken the precipitation growth process.

Because of the complex interactions among the production of heat and smoke by the fire, atmospheric motions, and the microphysical processes affecting the particles, modelling fire plume behavior is extremely difficult. A number of two-dimensional simulations of fire plumes have been conducted. These have been used to study the relationships among heat addition from the fire, production of buoyancy, generation of pressure gradients, and induction of fire winds, as well as the role of sub-grid turbulence and fire-plume radiation (Luti, 1981; Small et al., 1984a, 1984b; Proctor and Bacon, 1984). While these models have the advantage of high spatial resolution and give reasonable agreement with observations and experiments, they are not able to simulate the complex relationships between plumes and the ambient atmosphere which occurs within a three-dimensional framework.

A more realistic simulation of the plume development in the ambient atmosphere can be performed using three-dimensional cumulonimbus models, although these models suffer from a coarser resolution and do not include fire-plume radiation effects. Over the past decade, three-dimensional models have been quite successful in simulating the observed characteristics of cumulus and cumulonimbus clouds (Miller and Pearce, 1974; Cotton and Tripoli, 1978; Klemp and Wilhelmson, 1978a,b; Schlesinger, 1978; Clark, 1979; Tripoli and Cotton, 1980, 1985). Because of their superior representation of cloud dynamical processes, three-dimensional models have greater fidelity in simulating important interactions between the cloud and the surrounding environment than do numerical models in one- or two-dimensional frameworks. The three-dimensional models used to simulate fire plumes to date are the Colorado State University Regional Atmospheric Modeling System (RAMS) (Tripoli and Cotton, 1982; Cotton et al., 1985) and the model of Penner et al., 1985; (see also Haselman, 1980). Both models include the predicted effects of latent heating. However, RAMS also predicts the growth and effects of ice and rain precipitation, which allows it to simulate the effects of buoyancy changes resulting from precipitation movement relative to the air parcel. This effect could be equivalent to as much as a 1–3°C temperature perturbation. For these studies, both models also predicted the evolution of a passive tracer representing smoke. The RAMS model also calculates the effects of thermophoretic, diffusiophoretic, and Brownian-induced scavenging by the simulated cloud and precipitation elements; a single-sized smoke (soot) particle with a radius of 0.1 μm is assumed. Because experimental evidence (Section 3.5) indicates that soot particles are generally poor CCN, nucleation scavanging was neglected by RAMS. However, some studies have found that smoke particles from forest fires do act as CCN (Radke et al., 1980b), implying that nucleation scavenging could prove to be an important removal mechanism.

RAMS was employed by Cotton (1985) to simulate a hypothetical post-nuclear-attack urban fire occurring in the early morning in Denver, Colorado on 4 June, 1983. On that day, sufficient moisture was available to trigger intense local thunderstorms. (In fact, strong thunderstorms actually were observed later that day.) The simulation was performed using three surface heat fluxes: 8×10^4 W/m^2 (intense), 4×10^4 W/m^2 (medium), and 0.8×10^4 W/m^2

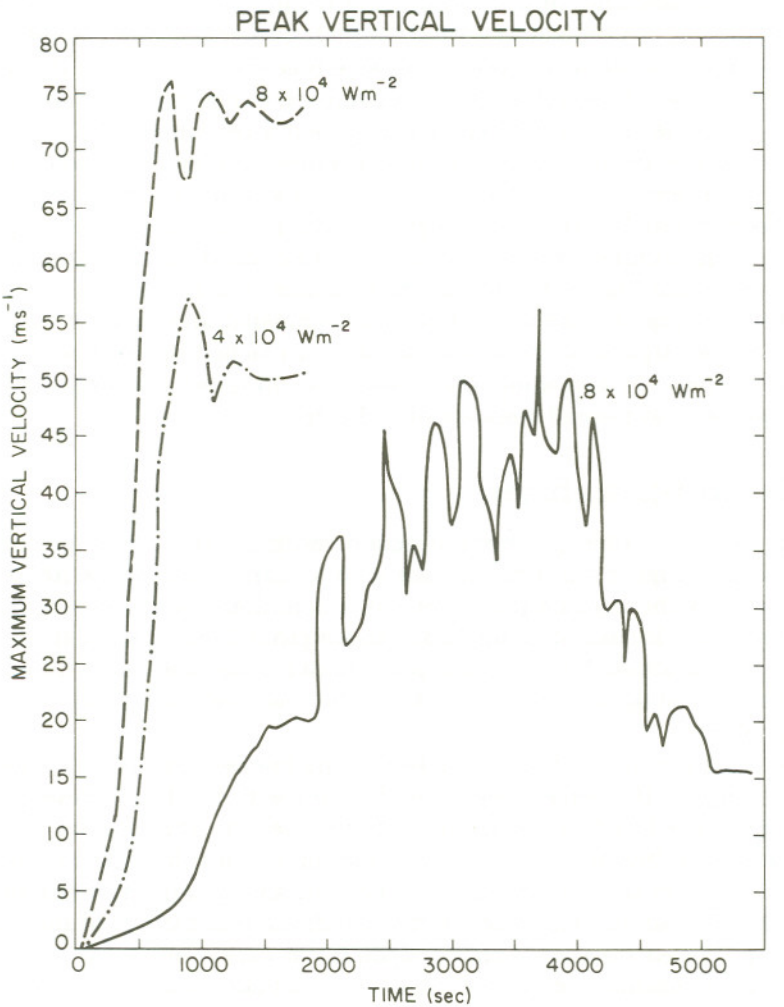

Figure 4.1. Peak vertical velocity in the simulated cumulonimbus cloud as a function of time for three different values of the fire heat source assumed by Cotton (1985). The curves are labeled with the source intensity and all fires cover a circular region with a radius of 4 km

(weak) applied over a circular region of 50 km^2. In each case, soot was injected along with the heat, assuming that 0.2% of the fuel is converted into soot. (In such tracer studies, the absolute amount injected is not critical since the tracer does not feed back into the rest of the model physics.) In addition to the water vapor entrained with the ambient air, water vapor released by fuel combustion was also included.

The intense case was found to produce a very strong updraft (Figure 4.1) that reached velocities of over 75 m/s and became nearly steady in time after 15 minutes of simulation. Within the updraft, temperature perturbations from ambient conditions of over 23°C were predicted. Because of the strong vertical motion, air parcels spent less than five minutes in the updraft before flowing into the anvil at 8–12 km above ground level. Since such a relatively short time was spent in regions of high condensation and large amounts of cloud water, less than 2% of the tracer aerosol was predicted to be removed by phoretic and Brownian scavenging (neglecting nucleation scavenging). The simulated plume produced an anvil that extended below and above the tropopause (see Figure 4.2) leading to maximum smoke and water detrainment in this region. The simulation was terminated after half an hour. By that time, no significant precipitation had yet reached the ground. Ice was deposited into the spreading anvil with concentrations reaching 6 g/kg of air, compared to normal amounts of 1–3 g/kg.

4.2.2 Smoke Injection Heights

The vertical profile of smoke injection resulting from the simulation is displayed in Figure 4.3. For the case with a heating rate of 8×10^4 W/m^2, over 50% of the injected tracer aerosol is deposited above the tropopause level, which is located at about 10 km above ground level. Another maxima occurs below about 2 km because some smoke is detrained and trapped at low levels. This appears in Figure 4.2 as the low-level, flange-like structure to the plume.

Reducing the fire heat source to half of the intense heat source produced little change in the percent injection of smoke with height. However, when the rate was reduced to one-tenth of the intense case, the resulting convection was noticably altered. In this case, the surface heat flux was insufficient to loft the tracer aerosol high enough to initiate strong condensational plume growth. After some time, precipitation did develop at the top of the plume which produced occasional strong updrafts in excess of 50 m/s. As a result, a weak maximum of aerosol injection eventually developed around the tropopause level (see Figure 4.3). There was also considerably more smoke deposited in the boundary layer in the first half hour (as is evidenced in Figures 4.2 and 4.3) for this weak intensity case than in the full and one-half intensity cases.

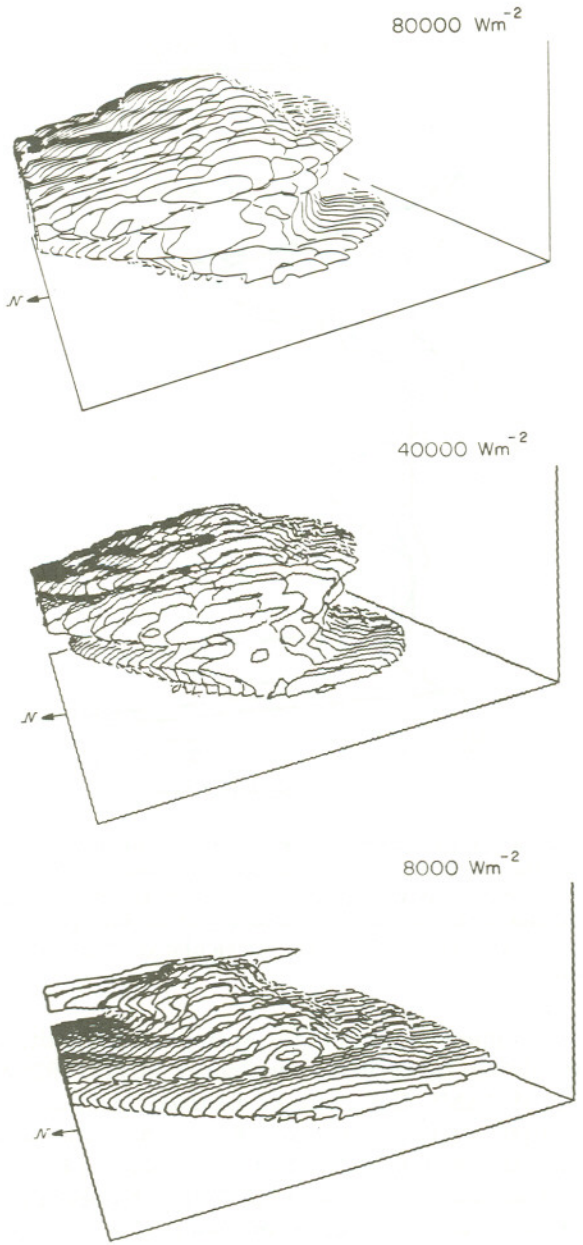

Figure 4.2. A three-dimensional depiction of the the exterior surface of the tracer aerosol cloud for the three values of the fire heat source assumed by Cotton (1985). The surface is the 10^{-8} g/m^3 contour level and the time is 30 minutes after the start of the calculation

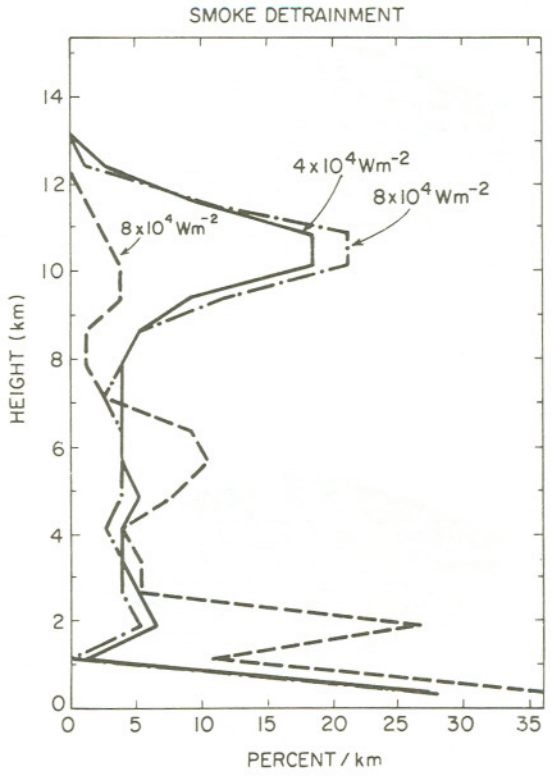

Figure 4.3. Vertical distribution of the tracer aerosol injection for the three different values of the fire heat source assumed by Cotton (1985). The horizontal axis is in units of percent of mass injected per vertical kilometer of atmosphere. The curves are labelled with the source intensity and all fires cover a circular region with a radius of 4 km. These numbers are calculated 30 minutes after the start of the calculation

Predictions of plume injection for spring/fall midlatitude standard atmospheric conditions were made by Penner et al. (1985) and by Banta (1985), who used RAMS. Both authors assumed a vertical shear with a unidirectional component and a horizontal flow with maximum speeds near the tropopause. Banta's peak horizontal wind was about 14 m/s, compared to a value of 18 m/s assumed by Penner et al. While Penner et al. assumed standard atmosphere relative humidities of about 77% at the surface decreasing to about 10% at the tropopause, Banta assumed 50% relative humidity throughout the entire depth of the atmosphere.

Penner et al. (1985) performed three simulations based on this thermodynamic profile. The first simulation considered a heat source of 8.9×10^4

W/m^2 (intense), the second simulation used a heat source of 2.3×10^4 W/m^2 (medium) while the third simulation used a heat source of only 0.23×10^4 W/m^2 (low). Each flux was specified over a circular region covering 78 km^2. Banta (1985) assumed a heat source of 9.4×10^4 W/m^2 over the same area. Using only that heat source, Banta (1985) performed three simulations. The first simulation considered moisture flux from the fire due to the release of water vapor by combustion in addition to the latent heat contained within the atmospheric water vapor in much the same manner as Cotton (1985). In the second simulation, Banta assumed no background atmospheric humidity in order to demonstrate the relative contribution of moisture released by the fire to plume penetration. Finally, in a third simulation, Banta removed all moisture effects in order to demonstrate the effects of only the fire heat to the plume rise.

The predicted smoke injections from all three simulations are displayed in Figure 4.4. Note that Banta (1985), who used RAMS, included only phoretic scavenging (which was less than 2% of the injected aerosol), while Penner et al. (1985) neglected all scavenging. Thus, both simulations treat the particles essentially as inert tracers. The predictions of Banta (1985) show the deepest smoke penetration with a maximum above the 11 km tropopause level for the case including natural and fire-induced moisture. The other two RAMS simulations demonstrate that the moisture from combustion is of only minor importance, but that the ambient moisture is of major importance. Even with the intense heat source considered, the majority of the smoke particles were detrained between 4 and 5 km when atmospheric moisture was omitted.

The most intense case simulated by Penner et al. (1985) resulted in a lofting maximum some 2 km in altitude lower than that predicted by Banta (1985). The most probable reasons for the difference between the results are that Banta initialized with greater moisture and that Penner et al. neglected the weight loss to the air parcel resulting from precipitation. A third factor which may bear on the difference is the diffusion of energy and aerosols within the models. In RAMS, the aerosol tends to be detrained at the highest level to which it is carried; in the Penner et al. model, the aerosol tends to overshoot its equilibrium level and then subside to the level at which it subsequently detrains. The cause of these differences is not understood. The Penner et al. results for the medium and low intensity cases demonstrate that, as the heating is reduced, the detrainment maximum quickly drops down to the 1–3 km level. This is consistent with the previously discussed simulations of Cotton (1985).

The results of these plume simulations suggest strong sensitivity of the height of smoke injection to the natural environment and to the intensity of the fire itself. This implies that atmospheric smoke injection resulting from a nuclear exchange would necessarily depend on the details of the atmospheric environments at the times and places that the fires occur. The

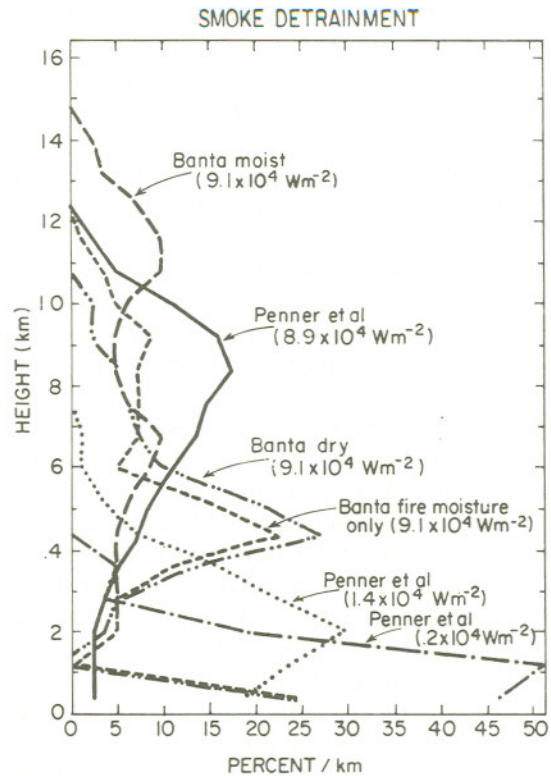

Figure 4.4. Vertical distribution of the tracer aerosol injection for the calculations of Banta (1985) and Penner et al. (1984) for the values of the fire heat source and for the moisture assumptions indicated. The horizontal axis is in units of percent of mass injected per vertical kilometer of atmosphere. These values are based on distributions 30 minutes after the start of the calculations

smoke injection profile that would arise statistically would most strongly depend on the time of the year. During the summer months, many of the likely strategic targets would be within conditionally unstable or moist (and thus potentially conditionally unstable) environments. For such targets, even the relatively small fires (less than 10^6 MW) could potentially lead to intense cumulonimbus clouds that could loft as much as 50% of the smoke into the upper troposphere and lower stratosphere, assuming minimal precipitation removal due to nucleation scavenging or hydrodynamic capture.

In less conditionally unstable but moist environments, intense cumulonimbus clouds would occur only over the larger fires. However, even in these environments, some smoke injection into the stratosphere is possible. In general, the ambient surface temperature would be less important than the available ambient moisture and the temperature aloft, because the heat

necessary to initiate a plume would come from the fire. Therefore, during the summer months, the average smoke injection profile for urban fires with heat releases greater than 10^6 MW will likely show a relative maximum near the average tropopause level.

During spring the atmosphere locally can be more conditionally unstable, but statistically is probably less favorable to deep convection than in the summer because of frequent stabilizing temperature inversions, lingering stable cold air regions, and drier air masses. The fall season would be even less favorable for the development of deep convection because of the existence of more warm air aloft and drier surface conditions. The winter season would be least favorable to deep penetration by fire-induced cumulonimbus clouds because of generally stable and dry conditions.

Overall, the model results suggest that the immediate lofting by plumes could inject, on the average, 50% of the smoke produced by intense post-nuclear-attack fires to within 3 km of the original tropopause during the summer months. The remainder would be injected at lower altitudes and, in part, removed by precipitation. The fraction lofted during spring and fall could be substantially less, and little would be injected at the tropopause level during the winter months. It is possible, that if nucleation scavenging or hydrodynamic capture were effective, the above estimates of lofting could be reduced, although it is impossible at this point to say by how much. The various studies of nuclear war effects (e.g., Turco et al., 1983a; NRC, 1985; Crutzen, et al., 1984) have assumed that the precipitation scavenging fraction is on the order of 30 to 50%. This estimate takes into account precipitation scavenging from all fires, including those that do not create strong convection.

4.3 MESOSCALE RESPONSE

Beyond the scale of individual fire plumes, the response of the atmosphere would involve weather systems on the scale of 100–1000 km. This scale is referred to by meteorologists as the meso-alpha scale (Orlanski, 1975). Following a major nuclear exchange, large amounts of smoke and, for moist convection, ice would be deposited in the upper levels of the atmosphere. Because smoke and ice are radiatively active in the visible and infrared parts of the spectrum, their presence could trigger meso-alpha circulations. Some preliminary meteorological evidence suggests that the radiative effects of cumulus anvils and the cooling effects of melting ice might drive meso-alpha convective activity. The effects appear to be stronger at night, perhaps due to lack of warming by sunlight at the anvil top, which may partially compensate for the longwave cooling at cloud top. Within soot-filled anvils, the diurnal variation of heating would probably be enhanced as a result of strongly increased solar absorption.

Observational evidence for the existence of meso-alpha systems of this type is found in a class of systems called Mesoscale Convective Complexes (MCCs) (Maddox, 1980). Occurring frequently over the Great Plains of the United States on summer nights, they seem to begin often as intense afternoon convective systems that initially produce a large ice anvil. Usually about 1–3 hours after sunset, these systems undergo a dramatic transformation from cellular convection into a large anvil system in which steady stratiform rain is the primary precipitation. Current theory suggests that long wave radiation and precipitation melting, in conjunction with a strong relative flow of low level moisture into the region, help organize the system. A similiar mesoscale weather system found in the tropics is called a tropical cloud cluster. W. Gray (personal communication) has also found that these systems have a similar strong diurnal variation.

As a result of geostrophic adjustment to anvil outflow, it has been shown that strong alteration of the upper level flow occurs in the region of an MCC (Maddox et al., 1981; Fritsch and Maddox, 1981). The result is the formation of mesoscale high pressure aloft in conjuction with a divergent anticyclonic outflow pattern. In the Northern Hemisphere, upper level jet streaks of up to 50 m/s form to the north west of the MCC at the 20 kPa (200 mb) pressure level. As low level moisture supplies are exhausted and the MCC weakens, elements of the upper level flow pattern can remain. The residual flow pattern seems to be capable of restarting the system when it again encounters favorable conditions (Cotton et al., 1982).

Because fire induced cumulus plumes have been shown by model results to cause significant anvil outflow of ice, smoke, and air mass, a meso-alpha system similiar to a MCC could result. In regions where urban strategic targets are clustered, the effect of merging anvils may be stronger. The large volume of ice deposited in these anvils must eventually precipitate or evaporate and would be likely to induce some motion due to the cooling at the melting or evaporating level. Large cooling rates due to infrared radiation divergence would be expected in the upper anvil, which, at night, could act to destabilize the upper anvil region. During the daytime, shortwave absorption by smoke mixed with ice would oppose such cooling, and could, in fact, dominate. The net radiative effect at this time is unknown. Given that such systems are observed and that some of the known conditions would exist in fire-induced cumulonimbus systems, a mesoscale response may be expected to occur. If so, the induced mesoscale circulation could redistribute the smoke vertically and horizontally from the regions predicted by the three-dimensional cloud models. However, it is not yet known whether individual fire plumes could form anvils extensive enough to trigger MCCs.

The larger mesoscale anvil systems that might occur would contain large amounts of ice, possibly leading to light rain at the surface over

large regions for a day or so following the initial strong convection phase. This would provide a second opportunity for scavenging mechanisms to deplete the large smoke concentrations deposited throughout the atmosphere. The smoke would have aged so that precipitation scavenging could be more efficient. Since slow sublimation of the ice would be occurring, some ice thermophoretic scavenging could be expected. Due to the many complex physical processes involved, and the uncertain composition of the post-nuclear exchange anvil and the environment, it is impossible to estimate the amount of scavenging that might occur in this mesoscale phase.

When large ambient vertical wind shears are present over the fire zones, cohesive anvil systems would be less likely to develop. In that case, precipitation formed aloft could evaporate after falling into drier layers below. This would introduce cooling and cause some mesoscale circulation response, which could be effective in continued mixing and dispersal of lofted pollutants.

It is less likely that only small amounts of ice would be present and that moist processes could be neglected. Even so, the mesoscale distribution of soot and other pollutants could cause horizontal temperature variations. This could, in turn, induce mesoscale circulation fields, that would continue to disperse smoke horizontally and vertically.

Mesoscale circulations would already exist in conjunction with normal synoptic and mesoscale weather patterns. Vertical motions associated with such features as jet streaks and frontal zones would be effective in subsequent vertical transport and horizontal dispersion of the lofted pollutants. Certain deformation fields associated with normal weather patterns could be effective in organizing strong, local vertical transport of pollutants. In particular, the regions near frontal zones, where secondary ageostrophic circulations exist, would have the largest influence.

For smoke deposited in the lower troposphere, thermally-driven mesoscale circulations such as seabreezes (Pielke, 1974) and slope flows (Defant, 1951) could lead to the preferred transport of materials to regions of mesoscale rising and sinking motions. Often, such zones of mesoscale rising motion are associated with natural cumulonimbus systems (Pielke, 1974; Banta, 1982) that could act to loft the material into the upper troposphere.

There are several potentially important short-term effects of mesoscale circulations in redistributing smoke initially lofted by fire plumes. Overall, however, the circulations are likely to lead to increased dispersion both vertically and horizontally, as there are no circulations that can increase local aerosol concentrations. One possible exception is the creation of clear spots through precipitation scavenging, leading to an increase in "patchiness". Without better data on scavenging rates and modeling of the poten-

tial radiation effects on the circulations, it is difficult to assess the importance of such processes. Although the lower stratosphere is highly stable, radiative cooling in the ice anvil could generate sufficient instability to create large scale overturning. Some smoke and ice separation could occur at cloud top, which would leave some of the smoke behind in the stratosphere. Whether the mixture of smoke and ice could lead to net cooling or warming of the anvil during the daylight hours may have an important impact on the distribution of smoke in the upper troposphere and lower stratosphere.

Because of our limited understanding of mesoscale circulations and the lack of experience with plumes from large, intense fires, much of the preceeding discussion has been speculative. It is worth noting, as was done in Chapter 3, that there are observations of wildfire plumes which show that smoke can be transported over very long distances. Wexler (1950) described transport of smoke from fires in Alberta, Canada extending down into the U.S. and across the Atlantic to Europe. More recently, Chung and Lee (1984) used satellite imagery to track plumes from fires in this same area across Canada to the Atlantic coast and down across the Great Lakes to New York. Voice and Gauntlett (1984) also made use of satellite imagery to track plumes from the Australian bush fires of 1984 across the Tasman Sea to New Zealand. In these and in other cases, there is no evidence of induced mesoscale circulations. This may be because the fires were not sufficiently intense to generate cumulonimbus systems or because large wildfires typically burn under hot, dry, and windy conditions that do not favor the development of deep convection. In any case, it is clear that this scale of interaction deserves attention in future research programs.

4.4 SYNOPTIC SCALE RESPONSE

Scales of atmospheric motions between 1000 and 10,000 km are referred to as synoptic scales. Generally, synoptic systems are responsible for weather variations occurring over periods of 2–7 days. For example, mid-latitude cyclones and cold air masses are synoptic weather systems. These systems could potentially play an important role in redistributing, transforming, and removing the smoke particles, and, in turn, the smoke could modify these systems.

In the first few days after a nuclear exchange, cloud-scale and mesoscale processes could act to mix soot and ice throughout the troposphere and possibly into the lower stratosphere over much of the Northern Hemisphere. The fire plume models suggest that the depth of the initial lofting would be strongly dependent on local atmospheric conditions. It follows that destabilized regions on the synoptic scale, such as those having cold air advection aloft or positive vorticity advection at mid levels, would be characterized by

the deepest soot and ice penetration aloft. On the other hand, very stable air masses would lead to the highest smoke concentrations below 3–4 km with little ice deposited aloft. Subsequent heating by solar radiation might then act systematically to weaken or strengthen the system relative to its natural state. Obviously, the induced changes in the strength of the synoptic system would then affect the mixing of the smoke.

As discussed previously, the generation of anticyclones and elevated jet streaks by mesoscale systems could significantly alter the normal progression of local synoptic scale systems. The possible generation of extensive regions of cumulonimbus clouds in the aftermath of a concentrated nuclear exchange might have a similiar effect. If a particularly dense arrangement of targets, e.g., missile silo fields, happened to lie under a region of strong conditional instability, it is possible that intense outflow aloft could create an upper level ridge on the scale of one or two thousand kilometers. A flow perturbation of this scale could propagate well beyond the time scale of the initial forcing. In addition, instabilities in the flow or forced flows at a later time might lead to the growth of subsequent weather systems. It is difficult to be more precise about these effects because the understanding of the relationships between mesoscale and synoptic scale systems in the natural atmosphere is very limited.

If surface fires can indeed amplify an existing disturbance or create a new disturbance on the synoptic scale, it is likely that the disturbance would propagate for at least several days. It can be anticipated that air motions associated with such systems would most likely lead to enhanced dispersion of the smoke for several days following the nuclear exchange. Precipitation processes could also act on the same time scale to remove some of the smoke. In any case, the synoptic scale effects would depend sensitively on the weather patterns at the time of the nuclear exchange. A more precise understanding of these effects may be obtained through future regional scale atmospheric modeling studies.

4.5 INTERACTION WITH SOLAR AND INFRARED RADIATION

As discussed in the preceeding section, smoke and debris clouds produced by nuclear detonations and the attendant fires could be spread by plume rise and mesoscale circulations over large areas of the Earth on spatial scales of 100 to 1000 km. These large smoke clouds would then interact with a variety of physical processes which are important in determining the weather and maintaining the current climate. The most important interaction is that with the radiation fields, including both the absorption of solar radiation and the emission of infrared radiation. This section will be concerned with the direct interaction of the injected smoke and dust particles with these fields and the implications for the radiative budget of the atmosphere.

4.5.1 Solar Radiation

The immediate result of the injection of optically-thick aerosol clouds into the atmosphere is to alter radically the pattern of absorption of solar radiation in the Earth–atmosphere system. Under normal conditions, about 30% of the incident solar radiation is reflected by clouds and the surface, 25% is absorbed by the atmosphere, and 45% is absorbed at the surface. This energy absorbed by the surface is subsequently transferred to the atmosphere by latent heat (evaporation of water), sensible heat (warming of the atmosphere by contact with the warm surface), and infrared radiation. The atmosphere convectively transports the latent and sensible heat upwards, distribut es it horizontally by atmospheric motions, and ultimately radiates it back to space as thermal or longwave radiation. A schematic of the energy deposition and transfer is shown in Figure 4.5 (taken from Liou, 1980).

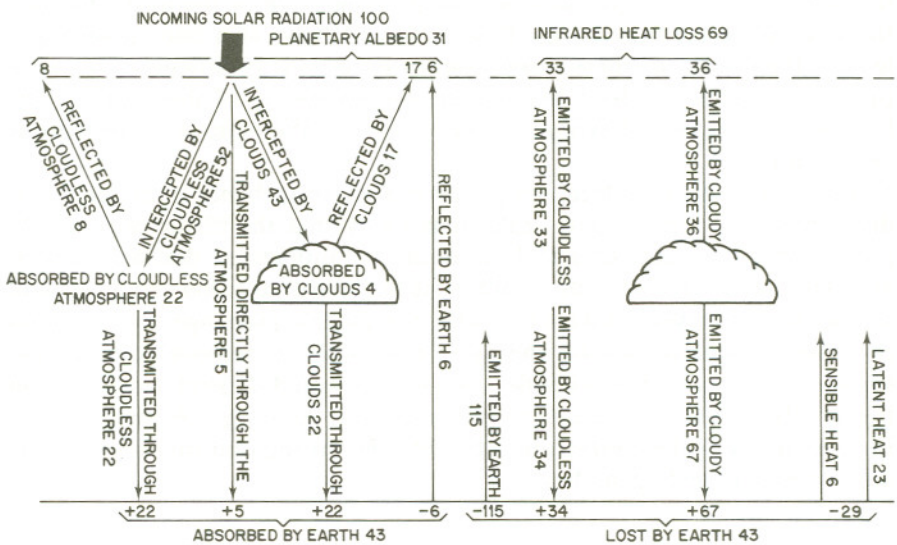

Figure 4.5. The heat balance of the Earth–atmosphere system for the present climate. Values are normalized to an incoming solar flux of 100 energy units (taken from Liou, 1980). Reproduced by permission of Academic Press

When an aerosol layer is introduced into the atmosphere, the direct solar beam is attenuated exponentially by the aerosol. The energy removed from the direct beam is partitioned into three categories: it may be absorbed by the aerosol particles, it may be scattered upward, or it may be scattered downward towards the surface. For most naturally-occurring aerosols such as cloud droplets, ice crystals, and wind-blown soil, downward-scattering dominates the other processes. Thus the basic effect of these aerosols is to

convert the direct solar beam to diffuse (scattered) solar radiation (hence, the white color of clouds). At the same time, some additional energy is scattered upwards and lost to space, thereby reducing the solar energy available to the surface-atmosphere system. The fraction of solar radiation reflected to space by the atmosphere and surface and lost from the system is called the planetary albedo.

If the smoke particles are assumed to contain an amorphous elemental carbon fraction on the order of 20% and have typical dimensions on the order of 0.1 μm to 1.0 μm, about half the extinction events (defined as a photon interacting with a particle) for photons at visible wavelengths result in the photon being absorbed by the particle. In contrast, for dust aerosols of the same size, about 2 in a 100 events result in absorption, and for pure water less than 1 in a million result in absorption. In addition, most of the scattering events, perhaps 7 out of 8, result in scatter towards the ground. Thus, for dust or water, the majority of photons continue on towards the Earth's surface after a single extinction event; for the smoke particles, only about half continue on towards the surface.

A quantitative comparison of the effect of nuclear dust and smoke aerosols on solar radiation is shown in Figure 4.6 (adapted from Turco et al., 1983a) where solar transmission (defined as the fraction of the incident solar energy that penetrates the aerosol layer as either direct or diffuse radiation) is plotted as a function of optical depth. For a given value of optical depth, the transmission through the dust is considerably higher than that through smoke. The direct beam transmission is the same in both cases. For dust, the great majority of extinction events lead to scattering, while in the case of the smoke, a little less than half of the extinction events lead to absorption. The amount of transmitted radiation can be related directly to this difference (see Section 3.7). Furthermore, it is this difference which is primarily responsible for the potentially large climatic effects that are discussed in Chapter 5.

The presence of an aerosol layer also affects the amount of solar radiation reflected by the surface–atmosphere system. In the event of a large-scale nuclear war, ground bursts of nuclear weapons could inject dust layers directly into the upper troposphere and lower stratosphere, and air bursts could ignite large fires that could create black smoke layers throughout the troposphere. Thus, the most probable initial distribution of aerosols would consist of a dust cloud essentially overlying a smoke cloud, but with some mixture of the two in the upper troposphere (and above water clouds). Incoming solar radiation would then first be scattered by the dust, and then strongly absorbed by the smoke layer. For smoke extinction optical depths on the order of 3 or more, the planetary albedo would be on the order of 10 to 15% (Turco et al., 1983b; Cess, 1985; Ramaswamy and Kiehl, 1985), as opposed to the normal, averaged value of 30% (see Figure 4.5). The addition of an

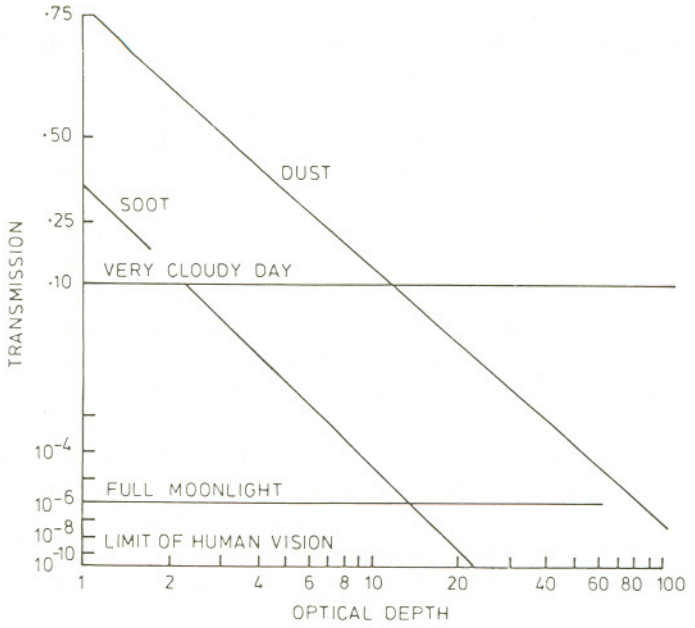

Figure 4.6. Transmission of solar radiation at 0.55 μm as a function of extinction optical depth for soot and dust aerosols. Size distributions and indices of refraction were taken from Turco et al. (1983b). Calculations were made with a multiple scattering model and assumed a solar zenith angle of 60°

overlying dust layer of optical depth 1 would increase the planetary albedo to a value of 20 to 25%, which is still less than that of the unperturbed planetary system. Thus, the Earth–atmosphere system could actually absorb more solar energy than in normal conditions. Despite this, the change in the height of the solar absorption leads to the apparently paradoxical cooling of the surface.

An illustrative calculation of solar transmission and reflection as a function of aerosol optical depth in an atmosphere containing no water clouds is given in Figure 4.7 (from Cess, 1985). The curves labelled Case II in the figure are for a smoke only layer (the smoke having a single-scattering albedo, ω—defined as the ratio of scattering to extinction—of 0.70 at 0.55 μm) distributed through the lower 75% of the atmosphere. Case I has the same smoke layer, but has a dust layer overlying the smoke. The dust layer has an optical depth equal to one-third that of the smoke and a ratio of scatter to extinction of 0.96. Case III is the same as Case I except two-thirds of the dust is mixed with the smoke and only one-third is above the smoke. For all three cases, the transmitted flux decreases steadily as the optical depth increases. For Case II (the smoke only case), the planetary albedo decreases with increasing optical depth, while for Case I it increases

due to the enhanced back-scatter by the dust. In Case III (which is not plotted) the reflected radiation is almost identical to that of Case II because only a small amount of dust overlies the soot.

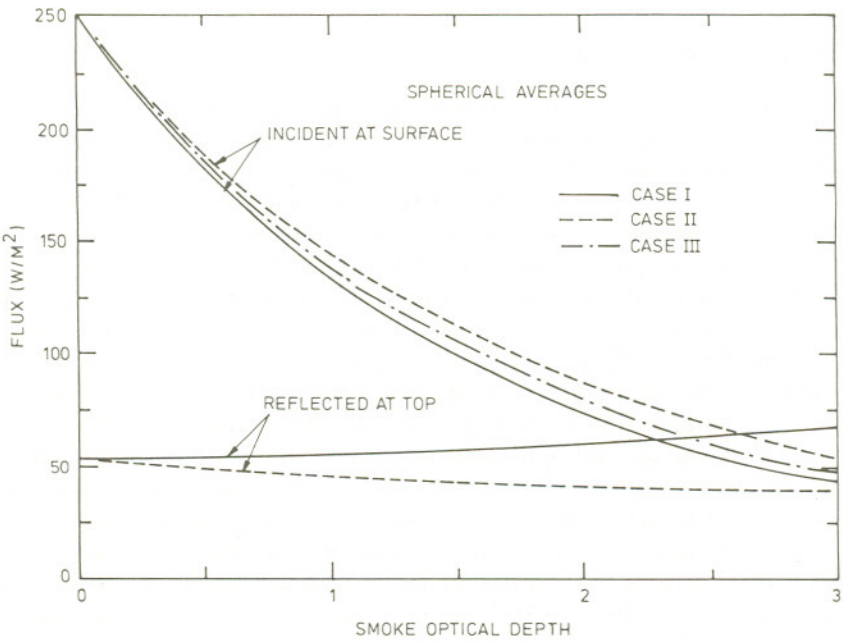

Figure 4.7. Spherically-averaged fluxes reflected at the top of the atmosphere and incident at the surface, as a function of extinction optical depth. Cases are explained in the text. The reflected fluxes for Cases II and III are virtually identical, so only Case II is shown (from Cess, 1985). Reproduced by permission of D. Reidel Publ. Company

As noted above and in Chapter 3, the transmission of solar radiation through an aerosol layer is determined in large part by the ability of the aerosols to absorb the radiation. In the calculations shown in Figure 4.7, Cess (1985) assumed that the smoke had a single-scattering albedo of 0.7. Turco et al. (1983a) and the NRC (1985) assumed a value of ω between 0.6 and 0.65, while Crutzen et al. (1984) assumed a value of about 0.4 (see section 3.6 for an extended discussion of smoke optical properties). If Cess had used a more absorbing smoke, (i.e., smoke with a lower single-scattering albedo), the transmitted solar radiation would have been reduced.

Calculation of the effects of aerosol particles on solar radiation, such as those shown in Figures 4.6 and 4.7, requires solution of the integral-differential equation of radiative transfer. Some of the multi-dimensional climate models which have been applied to the nuclear war problem use

approximate solutions which do not incorporate particle scattering. In order to treat this problem correctly, those models not now treating scattering will have to be modified; alternative approximate methods may also be suitable (Slingo and Goldsmith, 1985).

4.5.2 Infrared Radiation

As discussed in the earlier section on optical properties, the solar extinction (and absorption) optical depth of the smoke and dust aerosols is greater than the infrared extinction (and absorption) optical depth. This greater solar opacity has two immediate consequences. The first is that the climatological impact of a layer of absorbing aerosols is fundamentally different from that of greenhouse gases such as CO_2. These gases are primarily absorbers of infrared radiation. Increasing their concentration increases the infrared opacity of the atmosphere, which in turn warms the Earth's surface by making it more difficult for radiation to escape through the atmosphere. Aerosols, on the other hand, make it more difficult for the solar radiation to reach the surface. If the aerosols are non-absorbing, then the surface must cool regardless of aerosol optical depth because the aerosols will always act to increase the planetary albedo. For aerosols that absorb solar radiation, the surface will warm if the layer is near the surface and optically thin; it will cool if the layer is high or if the layer is optically thick. Detailed discussions of these various possibilities are found in Ackerman et al. (1985a) and Ramaswamy and Kiehl (1985). Even if the aerosol layer becomes optically thick at infrared wavelengths, the layer is generally optically thicker at solar wavelengths. The importance of this difference will be discussed in the next section.

The second consequence of the smaller infrared optical depth is that an optically thick aerosol layer must develop a temperature gradient. Solar heating of the layer occurs primarily between the layer top and the level at which visible optical depth 1 or 2 is reached. The layer's ability to cool by emitting infrared radiation is directly proportional to its ability to absorb infrared radiation, which is related to its infrared optical depth. This cooling from the layer top also occurs primarily in the region from cloud top to an infrared optical depth of 1 or 2. However, the thickness of this "infrared cooling" layer is greater than that of the "solar heating" layer because the infrared extinction cross-section per unit mass is smaller and, therefore, it takes more mass to reach the same optical depth. It follows that much of the infrared radiation originates well below the layer of solar heating. The greater thickness of the infrared emitting layer relative to the solar absorbing layer can be reduced by the presence of other infrared emitters such as water vapor and CO_2. However, due to the spectral characteristics of gaseous emitters, (i.e., the presence of infrared "windows"), these emitters

are generally not able to completely compensate for the difference in the aerosol optical depths at infrared and solar wavelengths.

As a result of this vertical distribution of heating and cooling, the smoke layer would develop a vertical temperature gradient with a maximum temperature at or near the layer top. This, in turn, would result in a stably stratified aerosol layer and inhibit mixing from below. This differential heating would only stop when the layer temperature becomes sufficiently hot that the emitted infrared energy from the layer top exactly matches the absorbed solar energy. However, long before this occurs, the heated air would mix upward into the ambient air above the layer, carrying the aerosol upwards. Obviously, the diurnally varying solar heating and relatively constant infrared cooling would result in diurnal variations in temperature at the top of the aerosol cloud. However, averaged over the daily cycle, the absorption of solar energy would dominate the emission of infrared energy.

In the preceeding discussion, the radiative concepts have been expressed in terms of the extinction optical depth of the aerosol. In reality, the more relevant quantity is the absorption optical depth, which determines the amount of incident radiation, either solar or thermal, absorbed by the layer. Because amorphous carbon is a highly absorbing material, the comparison of extinction optical depths between wavelength regimes is correct in a qualitative sense for smoke. However, for other materials such as water, which is transparent at solar wavelengths and has strong absorption features in the infrared, comparisons must be made on the basis of the absorptivity.

For absorbing particles that are small compared to the wavelength of the radiation being considered, absorption tends to dominate scattering. This fact can be used to derive an approximate method for treating the effects of aerosols on infrared radiative transfer. The aerosols are assumed to be absorbers only and scattering is neglected. In this case, the aerosols are essentially treated as a "gas" with an equivalent optical depth equal to the aerosol absorption optical depth as a function of wavelength. This approach, which simplifies the radiative calculations considerably, has been used without significant loss of accuracy in the studies by Turco et al.(1983a), Crutzen et al. (1984), and Haberle et al. (1985).

One situation that is likely to be important, and which cannot be treated by the absorption only approximation, involves the condensation of water on the smoke particles. As discussed in the section on mesoscale effects, following injection and the attendant initial precipitation, some layers might be saturated and condensation or freezing would occur on the particles, or smoke could be scavenged by water droplets or ice crystals, resulting in a polluted cloud or haze. Because of the large particle concentrations, the particles might only grow to sizes on the order of few microns in radius. However, this growth would still have an appreciable effect on the radiative properties of the aerosol, especially in the infrared. Due to the increase

in particle size by water condensation, the infrared extinction cross-section and optical depth would increase substantially. At the same time, the visible extinction optical depth would increase due to the increase in total aerosol mass, although the increase would not be as great as at infrared wavelengths. In short, if sufficient water were available for condensation, the infrared optical depth of the aerosol layer could become equivalent to the visible optical depth through particle growth. Since it is unlikely that enough water would be present to produce raindrops, the aerosol layer might resemble a haze layer rather than a typical stratiform cloud.

It should be clearly pointed out that these particles would be substantially different from normal haze or cloud droplets. Because of the inclusion of absorbing material within the droplet, they would have large absorption cross-sections even at visible wavelengths. In fact, the water could enhance the ability of the elemental carbon to absorb solar radiation, as has been shown theoretically by Ackerman and Toon (1981) and Chylek et al. (1984). (For an extended discussion of this problem, see section 3.6 on optical properties.) Therefore, it should not be concluded that the addition of water would allow the solar radiation to penetrate the aerosol layer; on the contrary, both extinction and absorption would likely be increased.

The GCM studies done to date have not included the effects of aerosols on the infrared radiative transfer, although they have been included in several of the one- and two-dimensional simulations. Neglecting the infrared effects presumably would cause the model surface temperatures to decrease too quickly and too deeply in the early period when both the visible and infrared aerosol optical depths are large. Although rapid cooling would be expected in any case due to the cutoff of solar radiation, increased infrared radiation from the aerosol layer could moderate the cooling rate, depending on the layer location and the initial temperature profile. This increased infrared emission from the layer may also act to cool the bottom of the layer more rapidly, which in turn may offset the moderating influence of the enhanced infrared emission at the surface. Including the infrared effects may also reduce the magnitude of the cooling somewhat if a considerable fraction of the injected aerosol is scavenged and removed rapidly from the atmosphere. Infrared effects would have only a minimal impact on the duration of the temperature perturbations (assuming that the smoke persists for periods of weeks or more), since the return to normal temperatures would be controlled mainly by the return of normal insolation levels, i.e., by the rate at which the smoke is gradually removed from the atmosphere. One further possibility is that the infrared effects would be important in regions such as the polar latitudes where there is minimal solar radiation. Infrared cooling may be especially significant in the polar night stratosphere where cooling might enhance downward motions, thereby aiding in the ultimate removal of the smoke.

4.5.3 Radiative Equilibrium

The effect of an aerosol layer on equilibrium planetary temperatures can be examined qualitatively using a simple model consisting of a black surface and a grey atmosphere (Ackerman et al., 1985a). In this model the atmosphere is assumed to be uniform in temperature, to be transparent to solar radiation (in the absence of aerosols), and to have an infrared gaseous emissivity of 0.8, which is roughly equivalent to the average emissivity of the Earth's atmosphere. A spectrally-grey aerosol that absorbs but does not scatter radiation is introduced into the model. The infrared absorption optical depth, $\tau_a(IR)$, is specified as a simple fraction of the solar absorption optical depth, $\tau_a(S)$, and equilibrium temperatures are then computed as a function of the solar absorption optical depth.

The results of this simple model, plotted in Figure 4.8, illustrate several of the points discussed in the preceeding two sections. As $\tau_a(S)$ increases, the equilibium surface temperature decreases, first slowly, then sharply in the region of $\tau_a(S)$ approximately 1. The decrease in temperature is a result of the reduction in solar energy reaching the surface. The slight increase in temperature at large $\tau_a(S)$ is caused by the aerosol layer becoming optically thick in the infrared. No temperature increase is seen in the case where $\tau_a(IR)$ is assumed to be 0.

As the surface temperature decreases, the atmospheric temperature increases as it absorbs an increasing fraction of the solar energy. For a layer that is optically thick at all wavelengths, both surface and atmospheric temperatures tend to the radiation-to-space temperature, which is defined as the average black-body radiation temperature necessary to emit to space the total solar energy absorbed by the surface–atmosphere system. For the Earth, the normal radiation-to-space temperature is about 254 K. Because this simple model has no vertical atmospheric structure, it cannot illustrate temperature gradient effects within the aerosol layer itself or within the atmosphere.

A similar analytical model has been used by Golitzyn and Ginsburg (1985) to obtain estimates of the surface temperature and mean atmospheric temperature of a planet for several different cases. The model gives reasonable results for both clean and dusty Martian atmospheres (Ginsburg and Feigelson, 1971; Ginsburg, 1973), for clean and dusty (due to an asteroid impact) terrestrial atmospheres, and for doubled CO_2 in the Earth's atmosphere. When applied to the nuclear war scenarios, the results are similar to those described above.

Both Crutzen et al. (1984) and Ackerman et al. (1985a) have extended these analytic equilibrium models to include a three-layer atmosphere. Although these models can be used to examine some of the effects of optically-thick aerosol layers of vertical temperature gradients, they are not capable

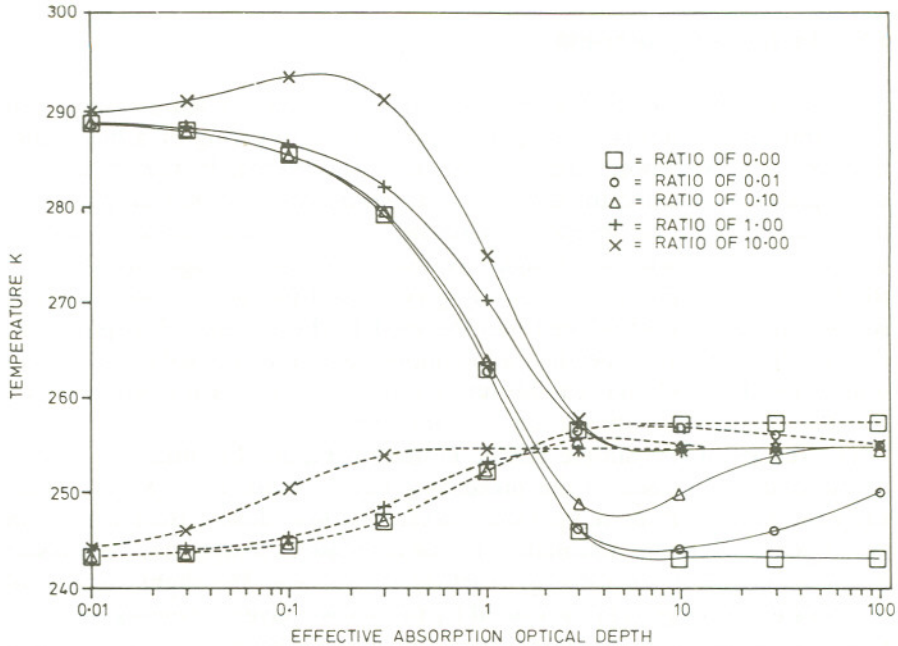

Figure 4.8. Equilibrium temperature as a function of the effective absorption optical depth for solar radiation (Ackerman et al., 1985a). The computations are from a one-layer grey atmosphere model. Solid curves indicate surface temperatures and dashed curves atmospheric (grey layer) temperatures. Symbols mark curves computed with different ratios of infrared to solar effective optical depth. Ratio values are shown in the legend

of adequately resolving temperature structure within the aerosol layer itself and therefore, still only provide approximate solutions.

While these simple models are limited in their vertical resolution and spectral detail, more realistic studies can be performed with one-dimensional radiative-convective models (RCMs). In addition to the more detailed radiative transfer calculations generally included in the RCMs, they also incorporate vertical structure and an atmospheric stability criterion. This criterion requires that when the temperature profile becomes unstable (i.e., when the vertical temperature gradient exceeds some critical value), the atmosphere is assumed to mix air upwards instantly to reduce the gradient back to its critical value. This type of climate model has been used in a variety of climate studies over the past 15 years (for a review of RCMs, see Ramanathan and Coakley, 1978). For the nuclear war climate problem, sensitivity studies of equilibrium responses have been carried out with RCMs by Ackerman et al. (1985a), Cess et al. (1985), and Ramaswamy and Kiehl (1985). The latter study presents results at 20 days after injection, which is essentially an equilibrium response of the model.

As discussed earlier in this chapter, various vertical distributions of the smoke have been postulated. Ramaswamy and Kiehl (1985) compared the effects of the same total amount of smoke distributed with a constant density between the surface and 10 km latitude (Profile D) and smoke distributed with an exponential scale height of 3 km (Profile M). The same amount of solar radiation is absorbed by both distributions, but the heating rate distributions are quite different. The "M" distribution has a broad maximum centered near 5 km, while the "D" distribution has a sharp maximum at the layer top (10 km). The equilibrium temperature profiles for these two cases, as well as for an unperturbed atmosphere, are shown in Figure 4.9. The "D" profile has a sharper and more elevated inversion and a considerably greater surface cooling (a temperature change of $-32°C$ as opposed to $-22°C$ for the "M" profile). Since the surface receives the same amount of solar radiation in both cases, the enhanced cooling is primarily the result of less downward infrared radiation reaching the surface for the "D" profile. This is in turn related to the height at which the maximum absorption of solar radiation takes place. The higher the level at which this absorption occurs, the less atmospheric gaseous infrared opacity lies above the layer. The gaseous opacity tends to trap the infrared radiation emitted by the layer (the greenhouse effect). Thus, when the layer lies above the bulk of the infrared opacity, it can more easily radiate the absorbed energy to space, and the total energy radiated by the layer, both upwards and downwards, is reduced. Ackerman et al. (1985a) essentially pointed out the same effect when they noted that for an aerosol layer of given optical depth, the higher the layer, the colder the equilibrium surface temperature.

Cess et al. (1985) used a 2-level RCM to study the sensitivity of the surface temperature to various aspects of the aerosol layer such as vertical distribution and optical depth. Their RCM incorporates the same vertical structure and boundary layer physics as are in the Oregon State University 2-level GCM (Ghan et al., 1982), but the solar radiation code has been replaced with a delta-Eddington scheme, and the hydrologic cycle has been replaced with an assumption of constant relative humidity. They found that, as opposed to results for forcing by CO_2 concentration changes or by changes in the solar constant, the sensitivity response to increasing aerosol concentrations is non-linear due to the convective coupling between surface and troposphere and to the exponential behavior of solar absorption. For tropospheric aerosol layers with small optical depths, sufficient solar radiation continues to reach the ground to convectively couple the troposphere and surface. As long as this coupling is maintained, the surface temperature and tropospheric temperatures remain essentially unchanged; both temperatures actually may increase if the planetary albedo is reduced as a result of the aerosol absorption, or may decrease if the albedo is increased due to aerosol scattering. However, under dense smoke clouds, the surface and

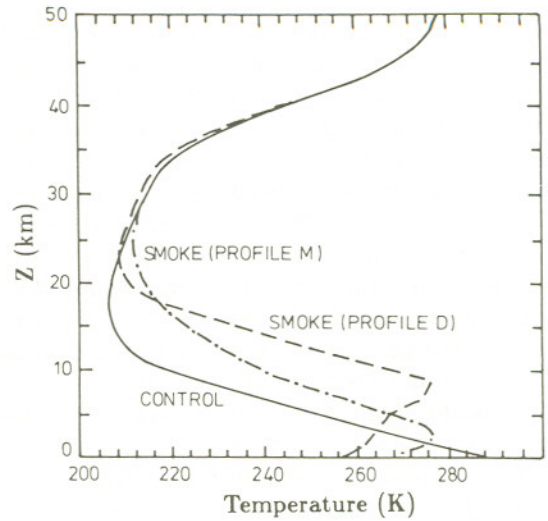

Figure 4.9. Thermal structure of the atmosphere for the unperturbed case, and for smoke profile M and smoke profile D. Temperature profiles for the smoke cases are for 20 days after the assumed injection (taken from Ramaswamy and Kiehl, 1985)

lower atmosphere can decouple due to a combination of increased stability in the middle troposphere and reduced heating at the surface, both of which suppress convection. As a result, the surface temperature can decrease dramatically because the direct solar heating is lost, mechanical transfer of heat from air to ground is suppressed, and the surface becomes very sensitive to small changes in the radiative forcing.

In addition to the RCM studies, Cess et al. (1985) were able to perform sensitivity studies with the OSU GCM, which was modified to include the delta-Eddington solar scheme. Their results show that, not unexpectedly, the surface cooling is sensitive to the layer optical depth, the aerosol single-scattering albedo, and the vertical distribution of the aerosol. The sensitivity to both the aerosol single-scattering albedo, ω, and the vertical distribution is demonstrated in Figure 4.10. As indicated, the visible extinction optical depth of the layer is 1. The changes in surface-air temperatures are computed over non-ocean areas only. The results of the change in vertical distribution are consistent with the RCM results discussed above and show that the decrease in surface–air temperature is more severe for more elevated smoke layers. As expected, decreasing the single-scattering albedo, which increases the absorption optical depth for a given extinction optical depth, also increases the severity of the cooling. The authors point out that the effect is more pronounced for the constant density distribution than for the constant mixing ratio distribution and attribute this difference to the greater effectiveness of surface–troposphere decoupling for the constant density case.

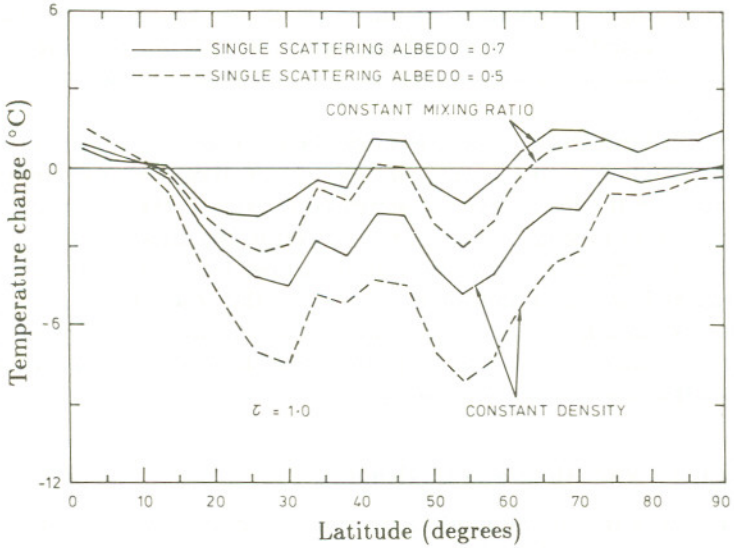

Figure 4.10. Zonally-averaged (over land and sea-ice areas) day 10 changes in July surface-air temperatures for changes of the vertical smoke distribution and the smoke single-scattering albedo, computed with the OSU 2-level GCM. The smoke optical depth is 1.0. (taken from Cess et al., 1985)

An important limitation of the studies by Cess and his colleagues may arise because of the vertical resolution of their models. The two model layers each are assumed to have equal atmospheric mass. Therefore, for the constant mixing ratio case, the optical depth is simply equally divided between the two layers. For the constant density case, approximately two-thirds of the smoke is in the upper layer and one-third in the lower layer. At these small absorption optical depths of 0.3 and 0.5 (for ω equal to 0.7 and 0.5, respectively) and for a constant mixing ratio distribution, roughly equal amounts of solar radiation are absorbed in each layer and each layer experiences roughly the same solar heating rate. Thus, both the change in overall atmospheric stability and the change in the average temperature of the lower layer are minimized, which also minimizes the surface-troposphere decoupling. If the absorption optical depth were greater, or if more of the aerosol were placed at higher levels in the atmosphere (as occurs in the constant density case), the solar heating per unit mass of air would be greater at the layer top, which would tend to heat the top layer preferentially and to stabilize the atmosphere, thereby increasing the decoupling of atmosphere and surface. In addition, since the bulk of the water is in the lower layer, the warmer temperature may increase the water vapor content, which would in turn increase the atmospheric opacity and the downward infrared radiation. Furthermore, the surface-air temperature is determined diagnostically, in part,

from the average temperature of the lower layer. All of these biases tend to reduce expected decrease in surface and surface-air temperature resulting from the attenuation of solar radiation, and may in some cases actually force a warming.

In the constant density case, the upper layer absorbs approximately twice as much radiation as the lower, and thus heats about twice as much. The temperature of the lower layer is decreased relative to the previous case due to the reduction in solar absorption. As a result, the atmospheric stability is increased. The increased absorption in the upper layer also implies a greater sensitivity at low optical depths to changes in the absorption optical depth, (i.e., changes in ω), because, as ω is decreased, an increasingly greater fraction of the absorption takes place in the upper layer due to the exponential nature of the attenuation of solar radiation.

4.5.4 Diurnal Variations and Daylengths

The majority of climate models are run with diurnally-averaged solar insolation. This means that the solar radiation is computed at a single value of the solar zenith angle chosen to approximate an exact average for insolation at the top of the atmosphere over daylight hours; this "averaged" solar radiation is then further multiplied by the fraction of the day during which the sun shines, and the result is used as the solar energy input to the climate model. While this is done primarily to increase computational speed, it has been assumed to introduce relatively little error in the values of daily average surface temperature predicted by the models. The success of this approximation is basically due to the fact that, under normal conditions, about two-thirds of the solar radiation absorbed by the surface-atmosphere system is deposited at the ground. Thus, most of the diurnal variations in the atmosphere on the scale of typical general circulation model grids are confined to the boundary layer (the lowest few kilometers of the atmosphere) and have relatively little impact on the predicted temperatures and wind fields at higher levels. However, it obviously has a substantial impact on the variables at the surface and precludes the calculation of diurnal variations in such quantities as surface temperature and evaporation rates.

In the case of optically-thick, elevated aerosol layers, this approximation would not be valid. The aerosol layer itself obviously would experience strong diurnal variations in solar heating, which presumably would lead directly to variations in the predicted model quantities. To date, the effects of such variations have not been studied in any detail, although several model runs with a diurnal cycle have been carried out using the 2-level OSU/GCM (Cess, personal communication; MacCracken and Walton, 1984). Unfortunately, however, comparisons of otherwise identical cases but with and without diurnal cycles have not been carried out.

An additional, and perhaps equally important, consequence of diurnally-averaged calculations was noted by Cess (1985). Because the solar radiation is attenuated exponentially by the aerosol layer, the effect of the solar zenith angle is very pronounced for layers with solar optical depths on the order of 1 to 3. The amount of sunlight reaching the surface on a daily basis can be substantially underestimated when an average solar zenith angle is used. Again, the climatological consequences of this underestimate have not been studied in detail, but it is assumed that this additional solar radiation reaching the surface will reduce the surface cooling somewhat. However, since heat transfer processes at the surface are highly non-linear, the magnitude of the reduction, or even if that reduction would occur, cannot be ascertained without further research.

TABLE 4.1.

DAYLENGTHS, IN HOURS, FOR A CLOUDLESS SKY AND VERTICAL AEROSOL EXTINCTION OPTICAL DEPTHS, τ, OF 0, 1.0, AND 3.0 AT A WAVELENGTH OF 0.55 μM. SUNRISE AND SUNSET WERE DEFINED TO BE THE TIME AT WHICH THE TOTAL DOWNWARD SOLAR FLUX AT THE SURFACE REACHED 10% OF NORMAL (CLOUD-FREE) NOON INSOLATION. THE AEROSOL SINGLE-SCATTERING AT 0.55 μM WAS ASSUMED TO BE 0.7

Latitude	$\tau = 0$	$\tau = 1.0$	$\tau = 3.0$
	A. Northern Hemisphere Summer		
60° N	16.0	11.8	4.1
30° N	13.9	10.9	7.6
15° N	12.7	10.1	5.5
0°	11.0	8.8	4.4
	B. Spring/Autumn Equinox		
60° N	11.0	7.5	–[a]
30° N	11.0	8.3	2.1
15° N	11.0	8.7	3.8
0°	11.0	8.9	5.1
	C. Northern Hemisphere Winter		
60° N	5.5	2.5	–[a]
30° N	8.5	5.1	–[a]
15° N	10.0	6.5	–[a]
0°	11.0	8.8	4.4

[a] Solar flux never exceeded the 10% normal criterion.

The effects of the smoke on normal diurnal variations in insolation may also be important for plant communities, many of which are highly sensitive to both the total amount of sunlight received and the period (the daylength) over which it is received (see Volume II of this report). The reduction in daylength due to absorbing aerosol layers with extinction optical depths of 1 and 3 and absorption optical depths of 0.3 and 0.9, respectively, were computed as a function of season and latitude. It was assumed that no water clouds were present in the atmosphere, and sunrise and sunset were defined as the time at which the solar insolation was one tenth of its normal, clear sky, noontime value. The results are given in Table 4.1. The daylength reductions are quite large, particularly at high latitudes, where the longer slant path of the solar beam becomes more important. In several instances, the solar flux reaching the surface never exceeds the one-tenth normal flux criterion.

4.6 INTERACTIONS WITH OTHER ATMOSPHERIC PROCESSES

As a result of the interaction of the smoke and dust with the radiation, various other atmospheric processes would be affected. The primary effect would be on the dynamical motions of the atmosphere, which would in turn influence the transport of the aerosols. There would also likely be significant alterations in boundary layer processes and in the hydrologic cycle. These interactions are described briefly in this section in a qualitative manner. More extensive discussions, particularly on the dynamical interactions and modifications to the hydrologic cycle are found in Chapter 5, where the results of the general circulation model studies are described.

4.6.1 Atmospheric Transport

Prior to studies of the smoke problem, the vast majority of studies of the transport of a trace species by atmospheric motions considered the trace species to be passive, i.e., to have no effect on the atmospheric motions. However, if a tracer has a significant effect on the distribution of radiative heating and cooling in the atmosphere, its presence will affect the motions of the atmosphere and, hence, its own transport. This is clearly the situation that arises when a layer of absorbing aerosols is present in the atmosphere.

From the previous calculations of the absorption of solar radiation by the smoke cloud, it can be inferred that the top of the cloud will heat and become buoyant, except perhaps during the winter season when insolation is weakest. As a result, the smoke would be lofted both by induced, small-scale convective motions and by the generation of large-scale upward vertical velocities. The extent of lofting would be directly related to the amount of available solar radiation, and thus (as already noted) would have a strong

seasonal and latitudinal dependence. In addition, the atmosphere is likely to develop a temperature inversion below the level of maximum heating which would act to reduce mixing from below. Wexler (1950) noted such an inversion in his study of the large smoke plume generated by forest fires in Alberta, Canada, in 1950 although the cause of the inversion could not be unambiguously determined. The combination of these two effects, lofting and stabilization, suggests that at least the upper part of the aerosol layer (absorption optical depth about 1) could be transported upwards and could stabilize the atmosphere below. In essence, this layer would form a stabilized "stratosphere", even if the smoke were not initially injected into the ambient stratosphere. For this reason the determination of the exact initial height of injection is perhaps less crucial than previously thought, although it still is likely to be an important factor in winter scenarios.

Inferences concerning subsequent smoke and dust transport can be drawn from observations of stratospheric winds and the transport of stratospheric aerosols. For a variety of reasons, including a reduced influence of both land-sea temperature contrast and topographical effects, stratospheric circulations tend to be strongly zonal, i.e., the flow around the Earth is along lines of constant latitude. Thus one might expect the lofted aerosols to be mixed fairly uniformly within latitudinal bands after a period of a few weeks. For example, Robock and Matson (1983) discuss the dispersion of the El Chichón volcanic debris cloud, which in the relatively weak zonal flow of the tropical stratosphere took about three weeks to form a band around the globe. In regions where no injection had occurred, atmospheric "eddies" would "diffuse" the material from other latitudes. This meridional spreading would presumably be somewhat faster in the case of absorbing smoke aerosols than in the case of non-absorbing volcanic aerosols due to the stronger temperature gradients produced by the smoke. The induced vertical motions would also lead to enhanced meridional dispersion due to strong wind-shear effects.

Obviously, the related issues of aerosol transport and modification of atmospheric dynamics and stability are a crucial aspect of the climatic impact problem being assessed here. The lifetime of the particles, which is discussed in more detail in Chapter 5, is highly dependent on atmospheric transport and thermal stability. In the current atmosphere, tropospheric particles tend to have lifetimes on the order of a few days to weeks, depending on their height and the local synoptic conditions. Stratospheric particles have typical lifetimes on the order of 6 months to 2 years due to the stability of the stratosphere and the lack of precipitation scavenging. The principal removal mechanism for stratospheric aerosols is, in fact, not direct removal, but injection of the aerosols into the troposphere, either through mid-latitude tropopause folding events or through migration to the winter poles and descent in the polar vortex, and subsequent removal from the troposphere by

scavenging. Since the particle lifetimes determine the longevity and severity of the climatological response, uncertainties in the smoke lifetimes in a modified atmosphere need to be reduced by further research.

4.6.2 Boundary Layer Processes

The impact of variations in climatologically-important parameters is usually quantified in terms of their effects on surface variables, particularly temperature. While this reflects primarily our bias as surface dwellers, it also reflects the important role that surface processes play in the planetary energy balance. Under normal conditions, the daily input of solar energy to the surface is nearly balanced by evaporative or latent heat transfer, turbulent conductive or sensible heat transfer, and infrared radiative exchange with the atmosphere. The relative importance of these terms, as well as the conduction of heat into the sub-surface, varies with season and location. Furthermore, there are obviously substantial differences between the thermal response of land and ocean surfaces. In the presence of an optically thick aerosol cloud, very little solar radiation will reach the ground; thus the focus of the present discussion will be on how the other terms in the energy balance might adjust to compensate for this loss of solar radiation.

4.6.2.1 Land Surfaces

For land surfaces, the effect of a thick smoke layer on the sensible heat flux is quite predictable. Due to the substantial reduction in insolation, the ground temperature quickly drops below the surface air temperature and an inversion forms. While this phenomenon occurs every night, the polar night provides a dramatic example of what can occur on longer time scales. Here the inversion deepens to a kilometer or more and the temperature difference over this layer may be as much as 15–20°C. As an example, a typical average temperature sounding for the month of February at Barrow, Alaska is plotted in Figure 4.11. Note the extreme stability of the lowest kilometer, which inhibits downward sensible heat transfer driven by mechanical turbulence.

Mechanical turbulence is produced by frictional drag on the winds at the Earth's surface. The drag generates vertical eddies that mix heat downward to the surface under stable conditions. Compared to buoyancy (which only mixes heat upwards from the surface), mechanical turbulence is a relatively poorly understood process dependent on the roughness of the surface and the local wind speed. As a general rule, the current generation of GCM's has incorporated rather simple boundary layer models. The ability of these current formulations to model adequately stable boundary conditions will have to be examined in view of the importance of these processes in determining the surface temperature. A correct determination of the downward heat flux

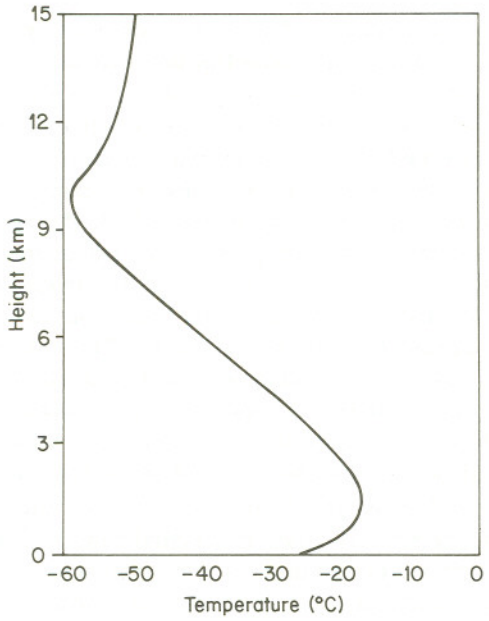

Figure 4.11. Monthly-mean temperature profile for February, 1978 at Pt. Barrow, Alaska

is especially critical at the very early times when the rate and magnitude of the surface cooling is likely to depend largely on the amount of heat that can be extracted from the atmosphere.

The role of evaporative cooling in the land surface energy balance most probably is reduced substantially under these conditions. For low or negligible insolation, evaporation must be strongly inhibited. During the initial transition period when the boundary layer is cooling, condensation would in fact occur. At the later stages, the low saturation vapor pressure of the cold boundary layer air would prevent much evaporation, even though water or ice is available at the surface. Given the low evaporation rates and the reduced convective mixing, a large reduction in precipitation rates over land would seem to be unavoidable. While transport of moist air from over the oceans to the land would occur, it is unlikely to compensate fully for the lack of evaporation and mixing. Overall, it seems plausible to conclude that latent heat would play a relatively unimportant role in the surface energy budget over land.

These qualitative conclusions concerning the surface energy balance are reinforced by the results of Covey et al. (1985), who present a more detailed analysis of the GCM model results reported in Covey et al. (1984). They point out that for land surfaces underneath an optically-thick aerosol layer, the moisture term in the surface heat budget actually becomes slightly

positive, indicating a net release of heat by condensation under these conditions. These calculations are discussed in more detail in Chapter 5.

Additional support is lent by the computations of Cess et al. (1985) with the 2-level RCM described in the section on radiative equilibrium models. The aerosol was assumed to be distributed between the surface and the model top (defined to be 200 mb) with a constant mixing ratio. The infrared opacity of the smoke was neglected. In the RCM, the surface is assumed to have no heat capacity, so an energy balance is determined by balancing absorbed solar radiation, net infrared radiation, and latent and sensible heat losses. As shown in Figure 4.12a, the solar radiation reaching the surface is reduced by the presence of an aerosol layer. The combined heat fluxes gradually decrease and eventually change sign. The small heat flux remaining for optical depths greater than 2.5 represents heat mixed to the surface by mechanical turbulence. The sum of this residual heat flux and the reduced solar radiation must be balanced by infrared losses from the surface.

Under normal conditions, the heat flux from, or into, the soil is relatively insignificant. Its primary role on seasonal time scales may be seen as controlling the amplitude of the diurnal temperature cycle. For soils which conduct heat poorly such as sand, little heat is stored in the soil and the diurnal amplitude is large. For soils such as clay or loam, the conductivity is higher, so the heat storage tends to reduce the diurnal temperature amplitude somewhat. Soil thermal conductivity is intimately related to moisture; wet soils are far more efficient heat conductors than dry soils. This suggests that should surface temperatures drop below freezing, the soil heat flux would decrease substantially. In short, the soil heat flux in soils with a high thermal conductivity may be an important factor in mitigating the surface cooling on the time scale of a few days. At longer time scales or for poorly conducting soils, it is unlikely to be significant.

The final energy component to be considered for the land energy balance is the downward infrared radiation. At first glance, one might expect this term to increase as a result of enhanced temperatures in the aerosol layer. However, the situation is more complicated. First of all, the majority of the downward infrared radiation reaching the surface under normal conditions originates in the relatively warm regions of the lower troposphere. If this layer cools as a result of an overlying aerosol layer, the downward infrared radiation reaching the surface actually decreases due to a reduction in the effective emission temperature of the lower atmosphere. Although radiation from the warm aerosol layer may partially compensate for this decrease, it is unlikely to do so completely unless the bulk of the aerosol layer is very low in the atmosphere.

This effect is demonstrated in Figure 4.12b, also taken from Cess et al. (1985). For uniformly mixed smoke at small optical depths, the net infrared radiation absorbed at the surface actually increases due to heating of

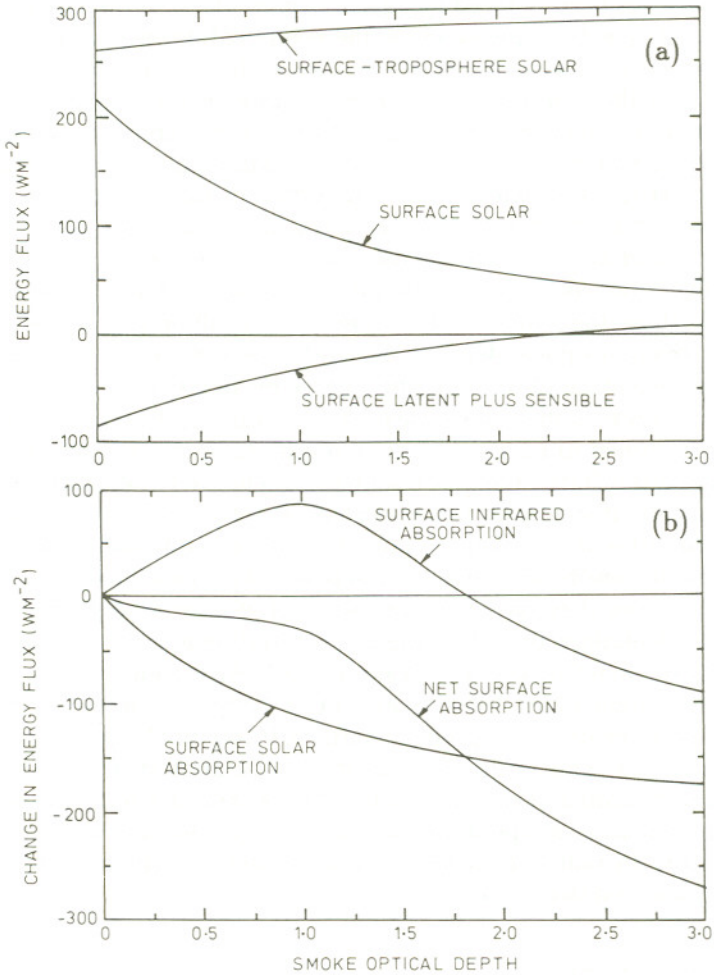

Figure 4.12. The equilibrium response (W/m^2) of a radiative convective model as a function of smoke extinction optical depth for (a) surface–troposphere solar absorption, surface solar absorption, and latent plus sensible surface heat flux; and (b) changes in surface solar absorption, surface infrared absorption, and net surface radiation absorption (taken from Cess et al., 1985)

the lower atmosphere. As the optical depth increases the net infrared begins to decrease and becomes a deficit at about optical depth 2. Taking into consideration that the ground temperature has decreased by 15°C at this same optical depth and, therefore, is emitting much less infrared radiation (since infrared emission by a blackbody is proportionally to the temperature raised to the 4th power, T^4), it is clear that the downward infrared flux from the

atmosphere has been reduced by a large degree. Because the model neglects the infrared opacity of the aerosols, the computed downward infrared radiation may be somewhat too small. However, this is probably only a small correction at these optical depths. Furthermore, as noted in the discussion on radiative equilibrium results, the uniform mixing ratio distribution of the aerosols assumed in the Cess et al. (1985) model places much of the smoke in the lowest few kilometers of the atmosphere, which in turn enhances the downward infrared radiation from clouds and the air to the surface.

Ackerman et al. (1985a) have also presented calculations illustrating this effect. Their results, in which the infrared opacity of the aerosol layer is included, show that, for radiative-convective equilibrium, a soot layer of visible extinction optical depth 3 located between 8 and 14 km can reduce the downward infrared reaching the surface by about 20% compared to the downward infrared flux under clear sky conditions. If the aerosols in this layer are assumed to have an infrared opacity equal to their visible opacity, the downward infrared remains essentially unchanged at equilibrium. Thus, while optically thin aerosol layers located near the surface may increase the downward infrared radiation reaching the surface, moderately thick layers in the middle troposphere or above are actually likely to reduce the downward infrared because they raise the effective level of solar absorption.

Model calculations that allow the aerosol heating to influence the dynamical motions (MacCracken and Walton, 1984; Aleksandrov, 1984; Haberle et al., 1985; Stenchikov, 1985; Malone et al., 1985; Thompson, 1985) show that the solar heating can produce vertical lifting of the particles and the surrounding air. This lofting reduces the temperature of the aerosol layer, through expansion and mixing, relative to the case of a fixed aerosol layer. Thus, the emission temperature of a smoke layer would be less than that computed from radiative-convective equilibrium, thereby reducing further the downward infrared flux.

4.6.2.2 Ocean Surfaces

Over the oceans, the situation would be quite different. Given the long thermal response time of the ocean mixed layer (generally the topmost 50 to 100 m of the ocean), the ocean surface will cool only very slowly when the insolation is removed. When cold air masses from land areas move out over the warmer oceans, strong air modification events with large upward fluxes of heat and moisture are to be expected. The depth of the modified air layer is difficult to specify from qualitative arguments. Although deep convection could be suppressed by the presence of an elevated inversion in the smoke layer, it seems plausible that a moderately deep layer of modified air with a thickness of a few kilometers might develop over the warm ocean.

There is, of course, considerable uncertainty in making the preceeding generalizations since the land and ocean cases have been considered as if they were unrelated. Obviously, the modification of continental air masses as they move offshore and the corresponding modification of marine air as it moves onshore need to be considered. While the uncertainties in predicting coastal effects are unlikely to be completely removed, our understanding of these effects can be enhanced through the use of appropriate numerical models and through the study of intense air modification events such as those which occur in the China Sea.

4.6.3 Hydrologic Cycle

Discussion of the qualitative effects of an aerosol layer on the hydrologic cycle is difficult because the hydrologic cycle is strongly dependent on both radiation and atmospheric dynamics. Some plausible arguments can be set forth but few can be stated definitively without further analysis. Consequently, the following discussion attempts to identify issues of importance.

The modification of condensation and precipitation processes would occur during both the transient phase and the quasi-equilibrium phase. Neglecting initial scavenging in the fire plume, which has been discussed elsewhere (Chapter 3), scavenging can occur by water vapor that has been redistributed by entrainment from the boundary layer to the middle troposphere or above. Considerable confusion has been generated on this issue because, on a gram per gram basis, more water vapor than aerosol is generated by combustion. The real issue, however, is the relative change in atmospheric water vapor concentrations produced by the injection. While background aerosol concentrations are typically small, water vapor column amounts are order of 10^4 g/m^2. In the NRC (1985) report, it was estimated that the average global water vapor concentration in the upper troposphere might increase by a maximum of 20% due to all the fires in a major nuclear war. As pointed out earlier in this chapter, this excess water vapor can be very important on a local scale in producing severe cumulonimbus storms with some attendant rainfall and particle removal. On the longer timescale and larger spatial scale, the effect of such an increase is uncertain. There will be some increase in infrared opacity and perhaps some residual ice crystals at the early times following injection. However, once the smoke begins to heat the air by absorbing solar radiation, the air will be well below saturation and condensation will cease in the aerosol layer (Covey et al., 1984; Malone et al., 1985).

A related issue that has received considerable attention by critics of the nuclear winter hypothesis is the scavenging of aerosols by condensation processes as the atmosphere cools beneath a smoke cloud (Teller, 1984; Katz, 1984). They have argued that as the atmosphere cools, condensation and

scavenging will occur. This condensation, however, is not likely to affect the upper levels of the aerosol layer, which are being heated. Also, this condensation would probably be analogous to nocturnal fog formation rather than to precipitating cloud formation. The amount of water actually condensing would be limited to the water vapor already in the air mass and would not result in large amounts of precipitation or efficient particle removal, although some coagulation might occur.

Possible changes in cloud optical properties also need to be considered. In an earlier section, it was pointed out that the inclusion of absorbing material in cloud droplets actually enhances the effective absorption of the material. In an atmosphere so impregnated with aerosols, it is difficult to imagine that any clouds would be formed that did not include a significant amount of absorbing material. Thus, the clouds which did form would be much more absorbing in the visible than present clouds. Furthermore, the presence of large numbers of aerosol particles would presumably lead to clouds with more but smaller droplets, which might increase the reflectivity of clouds (Twomey et al., 1984). Since absorption within the cloud would tend to decrease the reflectivity, the exact result would depend on the amount of absorbing material present within the cloud. In any case, either process would reduce cloud transmissivities, thus further reducing the solar radiation reaching the ground. Of course, significant absorption within the cloud would also act to evaporate the cloud.

Because of the physical complexity of the processes involved, modelling cloud formation in GCMs is a very difficult problem. Current schemes tend to be idealized and empirically tuned to the present climate, as they must be since the grid spacing in the climate models is much larger than the scale of individual clouds. Interactions with radiative transfer codes are carried out in a variety of ways, none of which are entirely appropriate for simulating the actual interactions. While some models do a fair job of predicting globally-averaged cloud statistics, regional-scale cloud predictions are often less successful and the precipitation predictions are often marginal. As noted before, clouds are the dominant removal mechanism for aerosols. Modelling the microphysics of particle scavenging is a difficult problem even within the context of very detailed cloud models. The problem has hardly even been addressed within GCMs with their coarse resolution and highly parameterized clouds (MacCracken and Walton, 1984 and Malone et al., 1985 represent the first attempts within the studies of nuclear weapons effects). In short, since the current schemes are not completely satisfactory for study of the present climate, they are likely to be inadequate for studying clouds, precipitation, and washout processes of smoke generated by a nuclear war.

Interestingly, this short-coming of the models may not be as critical in the study of the short-term effects as in the long term. The low relative humidities associated with the strong heating in the aerosol layer make the

issue of cloud formation relatively unimportant in the early stages. At later times as the smoke disperses and thins, cloud formation would again become a very important part of the climate simulation.

4.7 GEOPHYSICAL ANALOGUES

There are phenomena in nature where the aerosol interactions discussed in this chapter are of importance. To some extent these phenomena can, and have, been used both to validate climate models in general and to aid in understanding the climatological effects of a nuclear war. Several of these analogues will be considered briefly regarding their relevance to the present problem. One other, the possible impact of an asteroid causing the extinction at the Cretaceous–Tertiary boundary (Alvarez et al., 1980, 1984; Toon et al., 1982), will not be discussed since virtually no evidence on the atmospheric effects of such an event can be deduced without recourse to the very same models that are currently being used to study the nuclear effects problem.

4.7.1 Volcanic Eruptions

In 1783 Benjamin Franklin proposed that the volcano Laki which erupted in Iceland was responsible for the cold summer weather in Europe of that year. Humphreys (1940) was the first to examine the volcanic hypothesis quantitatively. Although his treatment was incorrect in several important aspects, it illustrated the potential for volcanic eruptions to affect global climate. The idea that large atmospheric injections of aerosol could cause extremely severe climatic perturbations was suggested by Budyko (1974), who considered the potential effects of several large eruptions occurring within a relatively short period of time. A recent review of the current status of our knowledge of volcanic effects was given by Toon and Pollack (1982). They concluded that large volcanic eruptions can affect the climate through the injection of gases leading to the formation of sulfuric acid droplets into the stratosphere. The ash particles injected by the volcanos are typically much larger in size and tend to settle rapidly out of the atmosphere.

While volcanic aerosol layers might appear to be reasonable analogues of those projected to be produced by nuclear detonations and fires, they are not. Sulfuric acid droplets have very different optical properties compared to smoke particles. Sulfuric acid droplets are essentialy transparent at visible wavelengths. Thus, their primary effect is to scatter solar radiation and thereby increase the planetary reflectivity (albedo). They do have appreciable absorption at thermal infrared wavelengths and can actually heat the stratosphere locally by absorbing upwelling infrared radiation emitted by the surface and lower atmosphere (Labitzke et al., 1983).

Furthermore, while the model predictions of the effect of volcanic aerosols are quite consistent in predicting a small decrease in surface temperatures over large spatial scales, this decrease has never been observed directly, although considerable inferential evidence is available that cool summers have followed large volcanic eruptions (Stommel and Stommel, 1983). Kelly and Sear (1984) claim that volcanic eruptions also may be responsible for declines in monthly mean land surface temperatures on the order of a few tenths of a degree in the several months following the eruption. On the local scale, Mass and Robock (1982) showed that diurnal variations in surface temperature were damped under the volcanic ash plume following the eruption of Mount St. Helens. Apparently the ash cloud cooled the surface by reflecting and absorbing solar radiation during the day and warmed the surface by increased emission of infrared radiation at night. This was, however, only documented for a few days following the eruption. Attempts to isolate temperature signals at later times both at the surface and aloft were unsuccessful, apparently because most of the large ash particles fell out within the timespan of a few days and the remaining sulfuric acid and ash particles dispersed too rapidly.

4.7.2 Dust Storms

Regional scale dust storms are a frequent phenomena on Earth, and can reach the global scale on Mars. Saharan dust storms containing as much as 8 million tonne of dust have been observed (NRC, 1985). These storms move out of west Africa, westward across the Atlantic as far as South America. They can generate optical depths at visible wavelengths as large as 1. Observations show that convection is suppressed underneath the dust cloud and direct atmospheric heating occurs within the cloud. Brinkman and McGregor (1983) reported on dust clouds over Nigeria with extinction optical depths up to 2, reductions of daily mean total solar radiation of up to 30%, and corresponding temperature decreases of up to 6°C.

Although the dust particles involved are usually considerably larger than typical smoke particles and much less absorbing, the available evidence shows a climatic response very similar to that proposed for optically-thick smoke clouds. The rapid decrease in surface temperatures, the heating of the atmosphere, and the suppression of convection are all consistent with the physical processes discussed in the preceeding sections.

A similar phenomena is observed on a much larger scale on Mars where dust storms originate in the Southern Hemisphere during its summer and occasionally spread globally in a matter of a week or two. Extinction optical depths can reach values on the order of 5 and surface cooling of as much as 10 to 15°C occurs (Zurek, 1982). The Martian dust is apparently more absorbing than typical desert sand on Earth and thus produces strong heating

in the Martian atmosphere. The somewhat smaller temperature reduction than would be predicted for the Earth under the same conditions is likely due to both the large infrared optical depth of the Martian dust and the much weaker greenhouse effect and colder surface in the unperturbed Martian atmosphere.

The effects of Martian dust storms on the dynamics of the atmosphere have also been observed. Data from the Viking Landers show that the normal cyclonic activity of the Martian atmosphere is suppressed when the dust is present (Ryan and Henry, 1979). Boubnov and Golitsyn (1985) proposed an explanation based on the suppression of baroclinic instability in atmospheric flows when the vertical stability of the atmosphere is increased. A similar suppression of synoptic-scale fluctuations was observed in the NCAR GCM in experiments with injected smoke layers performed by Thompson (1985).

While Mars lacks an ocean to moderate temperature changes, the periodic, large Martian dust storms offer perhaps the most convincing, although still imperfect, analogue to the projected atmospheric effects of a major nuclear war. The large surface coolings, the heating of the atmosphere, the global transport of the dust, and the suppression of baroclinic activity are all similar to, and consistent with, the computed effects of optically-thick smoke layers.

4.7.3 Smoke from Forest Fires

As noted previously, forest fires occasionally produce large amounts of smoke that can be transported over large areas. Examples of this include the plume from the Alberta fires reported by Wexler (1950), plumes from the large Australian bush fires of 1984 (Voice and Gauntlett, 1984), smoke from peat fires in the U.S.S.R. in 1972 which were reported to travel over 5500 km (Grigoryev and Lipatov, 1978), and plumes from recent fires in Alberta seen in satellite photographs (Chung and Le, 1984). In several of these events, temperatures under the smoke plumes were observed to be several degrees lower than forecast, presumably due to the obscuration of sunlight by the plume (Wexler, 1950). An early review by Plummer (1912) gives some very interesting historical information on forest fires that led to smoke transport over long distances in North America at the beginning of this century. For example, he reported that a large forest fire in Idaho in August, 1910, covering an area of 10^4 km^2, caused "dark days" to occur over a total area of more than one million square kilometers, so that artificial light had to be used even during daytime. He also wrote: "In connection with the 1910 phenomenon it was noted that a cool wave followed, passing eastwardly over the same area, but spreading further southward, which gave the lowest temperatures, with frosts, for the month of August". Because much of the available information on fire plumes is anecdotal, however, it is difficult to

extract a reliable, quantitative picture of smoke behavior. While the smoke produced by forest fires is generally less absorbing than that produced by urban fires, plumes from large fires clearly present research opportunities that should be exploited in the future.

4.8 SUMMARY

The introduction of an optically thick aerosol layer into the atmosphere would have a significant effect on most of the important physical processes in the atmosphere. Severe storms induced by the strong heating of the fires could produce local effects such as the Japanese black rain. These severe storms, particularly in the case of adjacent targets, could lead to mesoscale and synoptic-scale disturbances. The most immediate and obvious effect on longer timescales would be on the deposition of solar energy both aloft and at the Earth's surface. Owing to the size of typical smoke particles, the effect on infrared radiative transfer would be in general considerably less important. However, the infrared effects could be important in layers which are optically thick at infrared wavelengths, as well as in locations where condensation and transient cloud formation produced high infrared opacities. Modifications in solar energy absorption patterns could both increase the buoyancy at the top of smoke layers and the stability at the bottom. Altered heating patterns also would force a response in the atmospheric dynamics, which would, in turn, alter the vertical and horizontal distribution of the smoke. The effect of this coupling is difficult to anticipate from qualitative arguments and will have to be explored using three-dimensional models (see Chapter 5).

The changes in solar heating would also have large effects on the surface energy budget. If most of the incoming solar radiation were absorbed by the smoke, the boundary layer over land would change from being weakly unstable on average to being very stable. In this case, sensible and latent heat fluxes would be considerably less important than normally, and the dominant term in the surface energy budget would be infrared exchange between the atmosphere and surface. Under these conditions, the surface would cool dramatically. Over the ocean, large upward fluxes of heat and moisture would probably occur, causing intense modification of cold air masses moving offshore. Questions regarding the warming of land surfaces by marine air masses, and the generation of mesoscale storms along coastal margins cannot yet be answered.

The effect of smoke on cloud properties is similarly important but difficult to quantify. Beneath the aerosol the formation of ground fogs would be probable. However, these fogs, like those found in such locations as Fairbanks, Alaska during the winter, would be unlikely to have strong effects on surface temperatures. Cloud formation above the aerosol seems unlikely

but, if it occurs, might increase the downward infrared energy reaching the surface. There is the possibility of some cloud formation in the stratosphere because of the much larger than normal accumulation of water vapor. Water cloud optical properties would certainly change because of both the greater availability of cloud condensation nuclei and the inclusion of absorbing material in and between the cloud droplets. If the near-surface air cooled below freezing, damaging frost and ice could form on vegetation.

While some of the effects of smoke can be understood using simple models and straightforward physical arguments, many of the effects are highly non-linear and cannot be easily quantified. These effects must be determined through the use of sophisticated general circulation models or specialized meteorological models. The present generation of GCMs lack the ability to simulate a number of the important physical processes. In particular, radiative transfer codes and boundary layer parameterizations must be improved. The models must also incorporate interactive aerosol transport, as is the case now with several models. In addition, treatments of the hydrologic cycle and cloud formation must be examined to see if they are adequate for study of the nuclear war problem. This model evaluation and development cannot be accomplished on a short time scale. If the results are to provide reliable answers to the questions that have been raised, careful and systematic studies will need to be carried out in future years.